Vol.2, No.2, Page 124- 133, 2024 https://doi.org/10.59628/jast.v2i2.897 ISSN 2958-9568 JAST

SUN PUBLISHER

مجلة جامعة صنعاء للعلوم التطبيقية والتكنولوجيا
Sana'a University Journal of Applied Sciences and Technology
https://journals.su.edu.ye/index.php/jast/

Propagation intensity and phase distribution of a Partially Coherent Lorentz–Gauss Vortex Beam in a Gradient-Index Medium

Mohammed S. Qusailah [1], **Abdu A. Alkelly** [1*] and **Wafa'a A. Al-Bahry** [1]

[1] **Department of Physics, Faculty of Science, University of Sana'a, Sana'a, Yemen.**

*Corresponding author: a.alkelly@su.edu.ye

Abstract

The study focused on examining the characteristics of partially coherent Lorentz-Gauss vortex beams in a medium featuring a gradient refractive index. The study employed the ABCD matrix, deriving analytical expressions for the cross-spectral density function based on the extended Huygens-Fresnel principle and the relationship between the Hermitian Gaussian function and Lorentz distribution. The findings revealed that the topological charge, coherence length, and gradient refractive index coefficient are pivotal factors influencing the beam's behaviour in the medium. An increase in topological charge led to an expansion of the dark spot in intensity, while the gradient refractive index plays a crucial role in altering the size and shape of the intensity periodically in the medium and does not affect the dark spot in the middle of the beam. The findings from this study hold potential for applications in remote sensing and optical communications, making them valuable for further research endeavors.

Article Info

Keywords:
Partially Coherent, Lorentz–Gauss Vortex Beam, Gradient-Index Medium

Article History:
Received: 26-February-2024,
Revised: 27-March-2024,
Accepted: 7-April-2024,
Available online: 5 May 2024

1. INTRODUCTION

Lorentz-Gauss beams have revolutionized laser technology, opening up new possibilities in applications such as optical communications and remote sensing. These beams are generated by a single-mode diode laser and have been extensively studied in different mediums, including uniaxial crystals [1], turbulent atmospheres [2], through axicon optical system [3], and Kerr media [4]. With their unique properties, including a zero central intensity and a spiral wave-front structure, these beams have proven to be highly effective in their applications. By using a spiral phase plate [5], a Lorentz-Gauss vortex beam is produced, which has been extensively studied in different mediums, including turbulent atmosphere[5], and gradient-Index Medium[6]. Another crucial aspect of a light beam is coherence. Low-coherence laser beams, also known as partially coherent beams, exhibit a number of intriguing characteristics, most notably an extremely powerful self-reconstruction. There are a lot of partially coherent laser beams that have been studied, including the partially coherent rectangular multi-Gaussian Schell-model vortex beam[7] and the partially coherent Lorentz Gaussian vortex beam (PCLGV)[8]. The partially coherent Lorentz-Gauss vortex (PCLGV) beam passing through ABCD optical systems has been discussed in many works[1, 9]. For instance, studied Propagation of a Lorentz–Gauss vortex beam through a paraxial ABCD optical system [10]. The combination of the vortex and partially coherent light characteristics makes these beams ideal for use in optical communications and remote sensing. Researchers continue to explore and develop this exciting technology for new and innovative uses in the future [11].

The gradient-index medium has proven to be a versatile medium with numerous applications in fields such as optical communication, focusing and image formation, and optical fiber fabrication [12]. Scientists and researchers alike have been captivated by the unique self-focusing capabilities of the gradient-index medium, and as a result, there has been extensive research on its properties. The propagation characteristics of several model beams through GRIM have been studied in the last few years, including Bessel–Gauss beams [13], Lorentz-Gaussian vortex beams[6], vortex Hermite-cosh-Gaussian beams[14], Airy–Gaussian vortex beams[15], on-axis and off-axis Bessel beams[16], and Gaussian vortex[12]. Despite this, researchers are yet to conduct any studies on the propagation of partially coherent Lorentz-Gauss vortex beam (PCLGV) in a gradient-index medium (GRIN) [17]. This knowledge gap presents an opportunity for further exploration and could lead to the discovery of new properties and applications of GRIN, particularly in the fields of optics and communication.

The partially coherent Lorentz-Gauss vortex beam is introduced for the gradient-index medium, and this paper derives analytical propagation formula. To better understand these beams' behavior in different mediums, the focusing properties and cross-spectral density of the PCLGV beam in the GRIN medium are investigated numerically. In addition, the effects of gradient refractive index, coherence parameter, and topological charge on the phase distribution and intensity are studied. This research aims to provide a comprehensive perspective on the behavior of these beams in various mediums.

2. MODEL OF A PARTIALLY COHERENT LORENTZ-GAUSS VORTEX BEAM

At the source plane, the electric fields of the LGVB beam can be expressed as[10]:

$$E\left(r_0,0\right)=\frac{w_{0x}w_{0y}}{\left(w_{0x}^2+x_0^2\right)\left(w_{0y}^2+y_0^2\right)} \times \exp\left(-\frac{x_0^2+y_0^2}{w_0^2}\right)\times\left(\frac{x_0+iy_0}{w_0}\right)^M, \tag{1}$$

where $r_0=(x_0,y_0)$ is the position vector at the source plane z_0, w_{0x} and w_{0y} are the parameters related to the beam widths of the Lorentz part of Lorentz–Gauss vortex in the x and y directions, respectively, w_0 is the waist width of the Gaussian part of the Lorentz–Gauss vortex beam, and M is the topological charge of Lorentz–Gauss vortex beam. Based on the theory of coherence, the fully coherent beam can be extended to a partially coherent beam, and considering the generation of partially coherent beams, the cross-spectral density of the PCLGV beam generated by Schell-model sources at the plane z = 0 can be expressed as[18]:

$$\begin{aligned}W(r_{01};r_{02};0)&=\left\langle E\left(r_{01},0\right)E^*\left(r_{02},0\right)\right\rangle\\&=\sqrt{I(r_{01},0)I(r_{02},0)}\times\mu(x_{01}-x_{02},y_{01}-y_{02}),\end{aligned} \tag{2}$$

where $\mu(x_{01}-x_{02},y_{01}-y_{02})$ represents the spectral degree of coherence and is represented as follows:

$$\mu(x_{01}-x_{02},y_{01}-y_{02})= \exp\left[-\frac{(x_{01}-x_{02})^2}{2\sigma_x^2}-\frac{(y_{01}-y_{02})^2}{2\sigma_y^2}\right], \tag{3}$$

when σ turns into infinity, $\mu(x_{01}-x_{02},y_{01}-y_{02})=1,$ thus becoming

$$W(r_{01};r_{02};0)=\sqrt{I(r_{01},0)I(r_{02},0)}, \tag{4}$$

and when $r_{01}=r_{02}$ then

$$W(r_{01};r_{02};0)=I(r_{01},0) \tag{5}$$

Substituting Eq. (1) into Eq.(3), partially coherent Lorentz-Gauss vortex beam at the source plane can be expressed as[11]:

$$\begin{aligned}W(r_{01};r_{02};0)=&\frac{1}{w_0^{2M}}\frac{w_{0x}w_{0y}}{\left(w_{0x}^2+x_{01}^2\right)\left(w_{0y}^2+y_{01}^2\right)}\\&\times\exp\left(-\frac{x_{01}^2+y_{01}^2}{w_0^2}\right)\times(x_{01}+iy_{01})^M\\&\times\frac{w_{0x}w_{0y}}{\left(w_{0x}^2+x_{02}^2\right)\left(w_{0y}^2+y_{02}^2\right)}\\&\times\exp\left(-\frac{x_{02}^2+y_{02}^2}{w_0^2}\right)\times(x_{02}-iy_{02})^M\\&\times\exp\left[-\frac{(x_{01}-x_{02})^2}{2\sigma_x^2}-\frac{(y_{01}-y_{02})^2}{2\sigma_y^2}\right],\end{aligned} \tag{6}$$

Where σ_x and σ_y are the spatial coherence length in the x and y directions respectively . By considering in Eq.(6), the relation between the Hermite-Gauss function and the Lorentz distribution function [11]:

$$\begin{aligned}\frac{1}{\left(w_{0x}^2+x^2\right)\left(w_{0y}^2+y^2\right)}=&\\\frac{\pi}{2w_{0x}^2w_{0y}^2}&\sum_{m=0}^{N}\sum_{n=0}^{N}a_{2m}a_{2n}\\H_{2m}\left(\frac{x}{w_{0x}}\right)&H_{2n}\left(\frac{y}{w_{0y}}\right)\\\times\ \exp&\left(-\frac{x^2}{2w_{0x}^2}-\frac{y^2}{2w_{0y}^2}\right).\end{aligned} \tag{7}$$

Where H_{2m} and H_{2n} are the $2m$ and $2n$ order Hermite polynomial, and H_{2m} can be expressed as[19]

$$H_{2m}(x)=\sum_{L=0}^{m}\frac{(-1)^L(2m)!}{L!(2m-2L)!}(2x)^{2m-2L}. \tag{8}$$

Similarly, H_{2n} can be expressed as in Eq.(8), only m replaced by n. And the expanded coefficients a_{2m} can be rewritten as: [10]

$$a_{2m} = \frac{(-1)^m}{2^{2m-1}\sqrt{\pi}}\left\{\frac{1}{m!}\sqrt{\frac{\pi}{2}}\,\mathbf{e}^{(1/4)^2}\text{erfc}\left[\frac{1}{\sqrt{2}}\right] + \sum_{s=1}^{m}\frac{2^{2s}}{(2s)!(m-s)!}\left[\sqrt{\frac{\pi}{2}}\,\mathbf{e}^{(1/4)^2}\times \text{erfc}\left[\frac{1}{\sqrt{2}}\right] + \sum_{t=1}^{s}(-1)^t(2t-3)!!\right]\right\}. \tag{9}$$

where erfc $[x] = 1 - $ erf $[x]$, and with an increasing in numbers $2m$ the values of a_{2m} will dramatically decrease. Now, recalling the following equation [19]:

$$(x+iy)^M = \sum_{L=0}^{M}\frac{M!i^L}{L!(M-L)!}x^{M-L}y^L, \tag{10}$$

then , Eq.(6) can be rewritten as[11]

$$\begin{aligned}
W(r_{01};r_{02};0) &= \frac{1}{w_0^{2M}}\left(\frac{\pi}{2w_{0x}^2w_{0y}^2}\right)^2 \\
&\times \sum_{m_1=0}^{N}\sum_{n_1=0}^{N}\sum_{m_2=0}^{N}\sum_{n_2=0}^{N} a_{2m_1}a_{2n_1}a_{2m_2}a_{2n_2} \\
&\times \sum_{L_1=0}^{M}\frac{M!i^{L_1}}{L_1!(M-L_1)!}\sum_{L_2=0}^{M}\frac{M!(-i)^{L_2}}{L_2!(M-L_2)!} \\
&\times x_{01}^{M-L_1}y_{01}^{L_1}\times H_{2m1}\left(\frac{x_{01}}{w_{0x}}\right)\times H_{2n1}\left(\frac{y_{01}}{w_{0y}}\right) \\
&\times \exp\left[-\left(\frac{1}{2w_{0x}^2}+\frac{1}{w_0^2}\right)x_{01}^2-\left(\frac{1}{2w_{0y}^2}+\frac{1}{w_0^2}\right)y_{01}^2\right] \\
&\times x_{02}^{M-L_2}y_{02}^{L_2}\times H_{2m2}\left(\frac{x_{02}}{w_{0x}}\right)\times H_{2n2}\left(\frac{y_{02}}{w_{0y}}\right) \\
&\times \exp\left[-\left(\frac{1}{2w_{0x}^2}+\frac{1}{w_0^2}\right)x_{02}^2-\left(\frac{1}{2w_{0y}^2}+\frac{1}{w_0^2}\right)y_{02}^2\right] \\
&\times \exp\left[-\frac{(x_{01}-x_{02})^2}{2\sigma_x^2}-\frac{(y_{01}-y_{02})^2}{2\sigma_y^2}\right],
\end{aligned} \tag{11}$$

2.1. The propagation of a partially coherent Lorentz-Gauss beam in a Gradient-Index Medium

Based on the optical matrix , the paraxial propagation of the partially coherent Lorentz-Gauss beam in a gradient-index medium can be determined by the Huygens-Fresnel integral as[9]:

$$\begin{aligned}
W(r_1,r_2,z) &= \left(\frac{k}{2\pi B}\right)^2 \iiiint W^{in}(r_{01},r_{02},0) \\
&\times \exp\left[-\frac{ikA}{2B}\left((x_{01}^2+y_{01}^2)-(x_{02}^2+y_{02}^2)\right)\right. \\
&\times +\frac{ik}{B}(x_{01}x_1+y_{01}y_1)-\frac{ik}{B}(x_{02}x_2+y_{02}y_2) \\
&\times \left.-\frac{ikD}{2B}\left(\left(x_1^2+y_1^2\right)-\left(x_2^2+y_2^2\right)\right)\right]dx_{01}dy_{01}dx_{02}dy_{02},
\end{aligned} \tag{12}$$

where A, B, and D are optical matrix components that the optical medium determines, $k=\frac{2\pi}{\lambda}$ is the wave number, and λ is the wavelength of the incident light. Considering the case of the PCLGV beams propagating in the gradient-index medium with the refractive-index distribution is[12]:

$$n(r) \simeq n_0\left(1-\frac{1}{2}\beta^2r^2\right), \tag{13}$$

where β is a parameter associated with the parabolic dependence of the refractive index, n_0 is the refractive index at z axis , and r is the distance from the axis of symmetry, and can be expressed as $r^2 = x^2+y^2$, which is the radial component. The optical matrix connected with GRIM within the paraxial approximation is expressed by[13]:

$$\begin{pmatrix} A & B \\ C & D \end{pmatrix} = \begin{pmatrix} \cos(\beta z) & \dfrac{\sin(\beta z)}{n_0\beta} \\ -n_0\beta\sin(\beta z) & \cos(\beta z) \end{pmatrix} \tag{14}$$

By recalling the following formulas [19, 20]

$$\begin{aligned}
\int_{-\infty}^{\infty} x^n\exp\left(-px^2+2qx\right)\,dx &= n!\exp\left(\frac{q^2}{p}\right)\left(\frac{q}{p}\right)^n \\
&\times \sqrt{\frac{\pi}{p}}\sum_{k=0}^{\left[\frac{n}{2}\right]}\frac{1}{k!(n-2k)!}\left(\frac{p}{4q^2}\right)^k \\
&= \sqrt{\frac{\pi}{p}}2^{-n}i^n\exp\left(\frac{q^2}{p}\right)\times\left(\frac{1}{p}\right)^{0.5n}H_n\left(-\frac{iq}{\sqrt{p}}\right).
\end{aligned} \tag{15}$$

$$(a+b)^n = \sum_{L=0}^{n}\frac{n!}{L!(n-L)!}a^{n-L}b^L. \tag{16}$$

By Substituting Eq.(11) into Eq.(12). After doing straightforward and lengthy algebraic calculation, we can obtain:

$$\begin{aligned}
W(r_1,r_2,z) &= \frac{1}{w_0^{2M}}\left(\frac{k}{2\pi B}\right)^2\left(\frac{\pi}{2w_{0x}w_{0y}}\right)^2 \\
&\times \exp\left[-\frac{ikD}{2B}\left(\left(x_1^2+y_1^2\right)-\left(x_2^2+y_2^2\right)\right)\right] \\
&\times \sum_{m_1=0}^{N}\sum_{n_1=0}^{N}\sum_{m_2=0}^{N}\sum_{m_2=0}^{N} a_{2m_1}a_{2n_1}a_{2m_2}a_{2n_2} \\
&\times \sum_{L_1}^{M}\frac{M!i^{L_1}}{L_1!(M-L_1)!}\sum_{L_2}^{M}\frac{M!(-i)^{L_2}}{L_2!(M-L_2)!} \\
&\times W(x,z)W(y,z),
\end{aligned} \tag{17}$$

where the expression of $W(x,z)$ is given by:

$$W(x,z) = \exp\left[\frac{1}{a_x}\left(\frac{ik}{2B}\right)^2 x_1^2\right]\sum_{L=0}^{m_1}\frac{(-1)^L(2m_1)!}{L!(2m_1-2L)!}$$
$$\times\left(\frac{2}{w_{0x}}\right)^{2m_1-2L}\sqrt{\frac{\pi}{a_x}}\left(\frac{1}{a_x}\right)^{M-L_1+2m_1-2L}$$
$$\times\sum_{k=0}^{[\frac{M-L_1+2m_1-2L}{2}]}\frac{(M-L_1+2m_1-2L)!}{k!(M-L_1+2m_1-2L-2k)!}\left(\frac{a_x}{4}\right)^k$$
$$\times\sum_{s=0}^{M-L_1+2m_1-2L-2k}\frac{(M-L_1+2m_1-2L-2k)!}{s!(M-L_1+2m_1-2L-2k-s)!}$$
$$\times\left(\frac{ikx_1}{2B}\right)^{M-L_1+2m_1-2L-2k-s}\left(\frac{1}{2\sigma_x^2}\right)^s\sqrt{\frac{\pi}{b_x}}$$
$$\times\sum_{t=0}^{m_2}\frac{(-1)^t(2m_2)!}{t!(2m_2-2t)!}\left(\frac{2}{w_{0x}}\right)^{2m_2-2t} i^{M-L2+2m_2-2t+s}$$
$$\times\ 2^{-(M-L_2+2m_2-2t+s)}\left(\frac{1}{b_x}\right)^{0.5(M-L_2+2m_2-2t+s)}$$
$$\times\ \exp\left(\frac{c_x^2}{b_x}\right) H_{M-L_2+2m_2-2t+s}\left(\frac{-ic_x}{\sqrt{b_x}}\right), \tag{18}$$

in which a_x, b_x and c_x are given by

$$a_x = \frac{1}{2w_{0x}^2}+\frac{1}{w_0^2}+\frac{1}{2\sigma_x^2}+\frac{ikA}{2B}, \tag{19a}$$

$$b_x = \frac{1}{2w_{0x}^2}+\frac{1}{w_0^2}+\frac{1}{2\sigma_x^2}-\frac{ikA}{2B}-\frac{1}{a_x}\left(\frac{1}{2\sigma_x^2}\right)^2, \tag{19b}$$

$$c_x = \frac{1}{a_x}\left(\frac{ikx_1}{2B}\right)\frac{1}{2\sigma_x^2}-\frac{ikx_2}{2B}, \tag{19c}$$

The expression of $W(y,z)$ is given by

$$W(y,z) = \exp\left[\frac{1}{a_y}(\frac{ik}{2B})^2 y_1^2\right]\sum_{L=0}^{n_1}\frac{(-1)^L(2n_1)!}{L!(2n_1-2L)!}$$
$$\times\left(\frac{2}{w_{0y}}\right)^{2n_1-2L}\sqrt{\frac{\pi}{a_y}}\left(\frac{1}{ay}\right)^{L_1+2n_1-2L}$$
$$\times\sum_{k=0}^{[\frac{L_1+2n_1-2L}{2}]}\frac{(L_1+2n_1-2L)!}{k!(L_1+2n_1-2L-2k)!}\left(\frac{a_y}{4}\right)^k$$
$$\times\sum_{s=0}^{L_1+2n_1-2L-2k}\frac{(L_1+2n_1-2L-2k)!}{s!(L_1+2n_1-2L-2k-s)!}$$
$$\times\left(\frac{iky_1}{2B}\right)^{L_1+2n_1-2L-2k-s}\left(\frac{1}{2\sigma_y^2}\right)^s\sqrt{\frac{\pi}{b_y}}$$
$$\times\sum_{t=0}^{n_2}\frac{(-1)^t(2n_2)!}{t!(2n_2-2t)!}\left(\frac{2}{w_{0y}}\right)^{2n_2-2t} i^{L_2+2n_2-2t+s}$$
$$\times\ 2^{-(L_2+2n_2-2t+s)}\left(\frac{1}{b_y}\right)^{0.5(L_2+2n_2-2t+s)}$$
$$\times\ \exp\left(\frac{c_y^2}{b_y}\right) H_{L_2+2n_2-2t+s}\left(\frac{-ic_y}{\sqrt{b_y}}\right), \tag{20}$$

in which a_y, b_y and c_y are given by

$$a_y = \frac{1}{2w_{0y}^2}+\frac{1}{w_0^2}+\frac{1}{2\sigma_y^2}+\frac{ikA}{2B}, \tag{21a}$$

$$b_y = \frac{1}{2w_{0y}^2}+\frac{1}{w_0^2}+\frac{1}{2\sigma_y^2}-\frac{ikA}{2B}-\frac{1}{a_y}\left(\frac{1}{2\sigma_y^2}\right)^2, \tag{21b}$$

$$c_y = \frac{1}{a_y}\left(\frac{iky_1}{2B}\right)\frac{1}{2\sigma_y^2}-\frac{iky_2}{2B}, \tag{21c}$$

Equation(17) is the analytical expressions for a partially coherent Lorentz-Gauss vortex beam propagating in a gradient-index medium at the receiver plane z, and the derived equations can be used to determine the propagation characteristics of a partially coherent Lorentz-Gauss vortex beam propagating in a gradient-index medium. If we put $r_1 = r_2 = r$ in Eq.(17), the intensity of a partially coherent Lorentz-Gauss vortex beam propagating in a gradient-index medium can be obtained. The spectral degree of coherence for the laser beam given at the receiver plane z can be expressed as[21]:

$$\mu(r_1,r_2,z) = \frac{W(r_1,r_2,z)}{[W(r_1,r_1,z)W(r_2,r_2,z)]^{\frac{1}{2}}} \tag{22}$$

Inserting Eq.(17) into Eq.(22), one can calculate the spectral degree of coherence. Based on the obtained equations, the intensity and coherence properties of a partially coherent Lorentz-Gauss vortex beam that propagates in a gradient-index medium will be investigated in the following section.

2.2. Simulation and discussion

In this section, the average intensity, phase, and vortex properties of the partially coherent Lorentz-Gauss vortex beam propagating in the gradient index medium are analyzed and illustrated using Eq.(17). We get the intensity when we put $r_1 = r_2$ into Eq.(17), while we get the phase when we put $r_1 = r$ and $r_2 = 0$ into Eq.(17) . The global values of the parameters used for the calculations shown in Table 1.

λ	n_o	x	y	z	M
0.6	1.56	x	0	z	2
β	σ_x	σ_y	w_o	w_{ox}	w_{oy}
0.25	3	3	2	3	3

Table 1. The global values of the parameters used in this work unless otherwise stated in some parts of it. (μm unit, for parameters that have a unit of length).

Figure.1 investigates the evolution the normalized average intensity of a partially coherent Lorentz-Gauss vortex beams propagating in the gradient-index medium with different values of M at different distances . It can be found that a partially coherent Lorentz-Gauss vortex

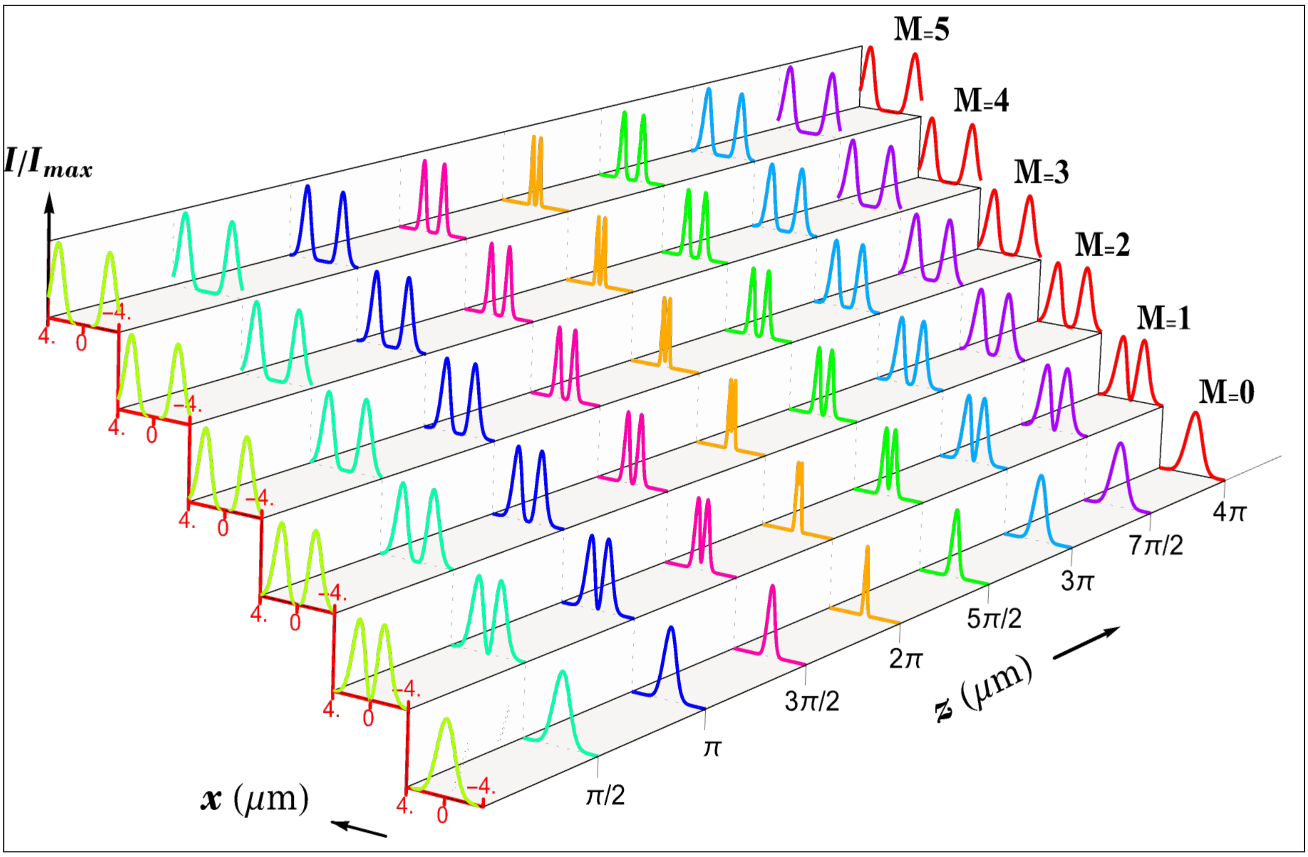

Figure 1. Cross section $(y = 0)$ of normalized intensity for partially coherent Lorentz-Gauss vortex beams propagating through the gradient-index medium with different values of M, at different distances.

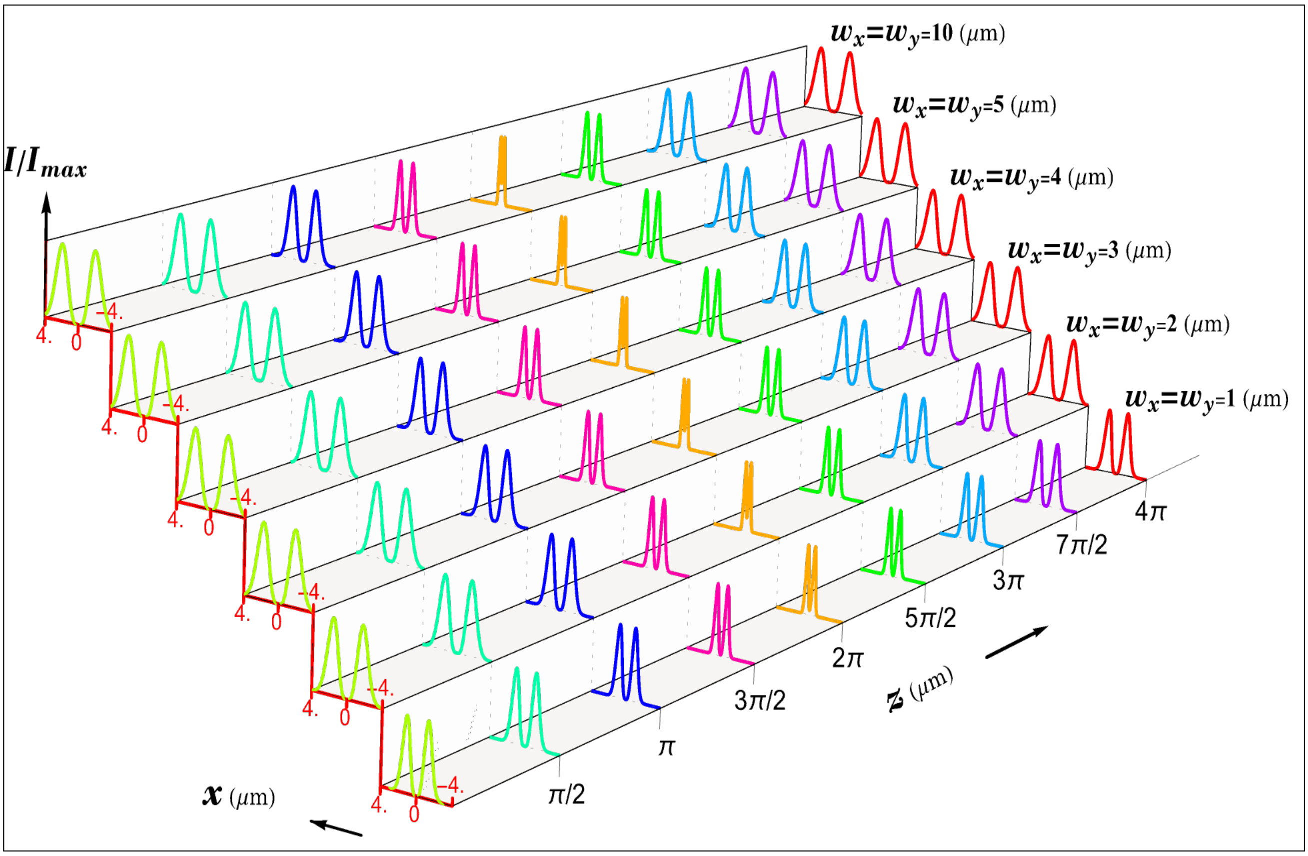

Figure 2. Cross section $(y = 0)$ of normalized intensity for partially coherent Lorentz-Gauss vortex beams propagating through the gradient-index medium with different values of $w_{0x} = w_{0y}$, at different distances.

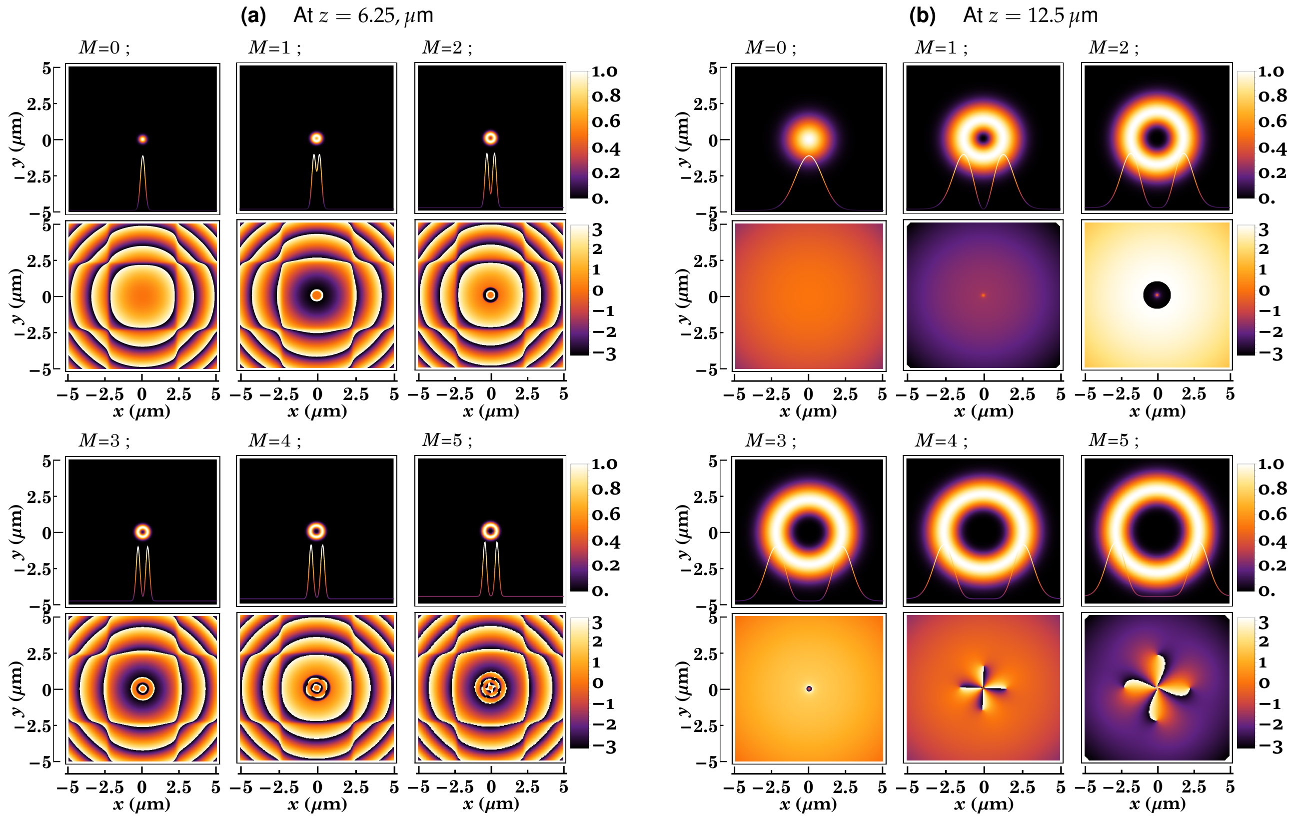

Figure 3. Normalized intensity and the phase distribution of the CSD function for partially coherent Lorentz-Gauss vortex beams propagating through the gradient-index medium with different values of $M = 0, 1 \ldots, 5$. At (a) $z = 6.25\ \mu$m, and (b) $z = 12.5\ \mu$m.

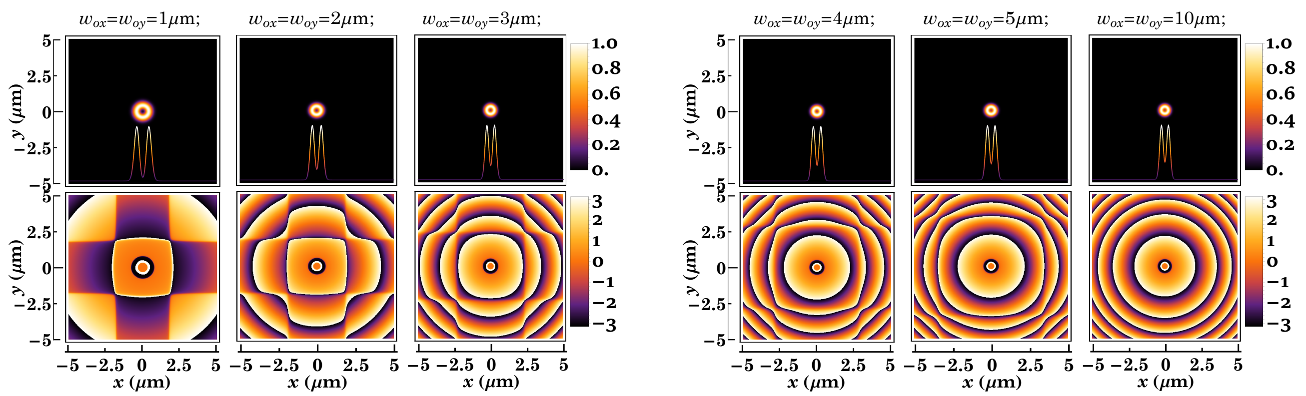

Figure 4. Normalized intensity and the phase distribution of the CSD function for partially coherent Lorentz-Gauss vortex beams propagating through the gradient-index medium With different values of $w_{0x} = w_{oy}$ at $z = 6.25\ \mu$m.

beam can keep its propagate periodically in the direction of z, and when $M = 0$, there is no dark spot in the middle, and the higher the value of M, the wider the dark spot and the greater the width of the beam.

Figures.3 show a cross-sectional view along the x-y axis for both intensity and phase. Fig.3a is observed that at $z = 6.25\ \mu$m, that the phase varies in evolution according to M, whether it is even or odd, where the dark spot in the middle of the beam represents the negative value of the phase when M is an odd number, and this spot decreases and the number of rings increases in its middle and takes a quadrilateral shape as the odd number of M increases, while the orange spot in the middle of the beam represents the zero value of the phase when M is an even number and this spot decreases and the number of rings around it increases with the increase of the even number of M. However, fig.3b is observed that at $z = 12.5\ \mu$m when $M = 0$, the phase is equal to zero, and as M increases, the number of rings increases, and these rings merge to form four petals when $M = 4, 5$, and the size of the petals is greater at $M = 5$ compared to $M = 4$.

Figure.2 describes the evolution of the normalized average intensity of partially coherent Lorentz-Gauss vortex beams propagating in the gradient-index medium with different values of $w_{0x} = w_{oy}$ at different distances.

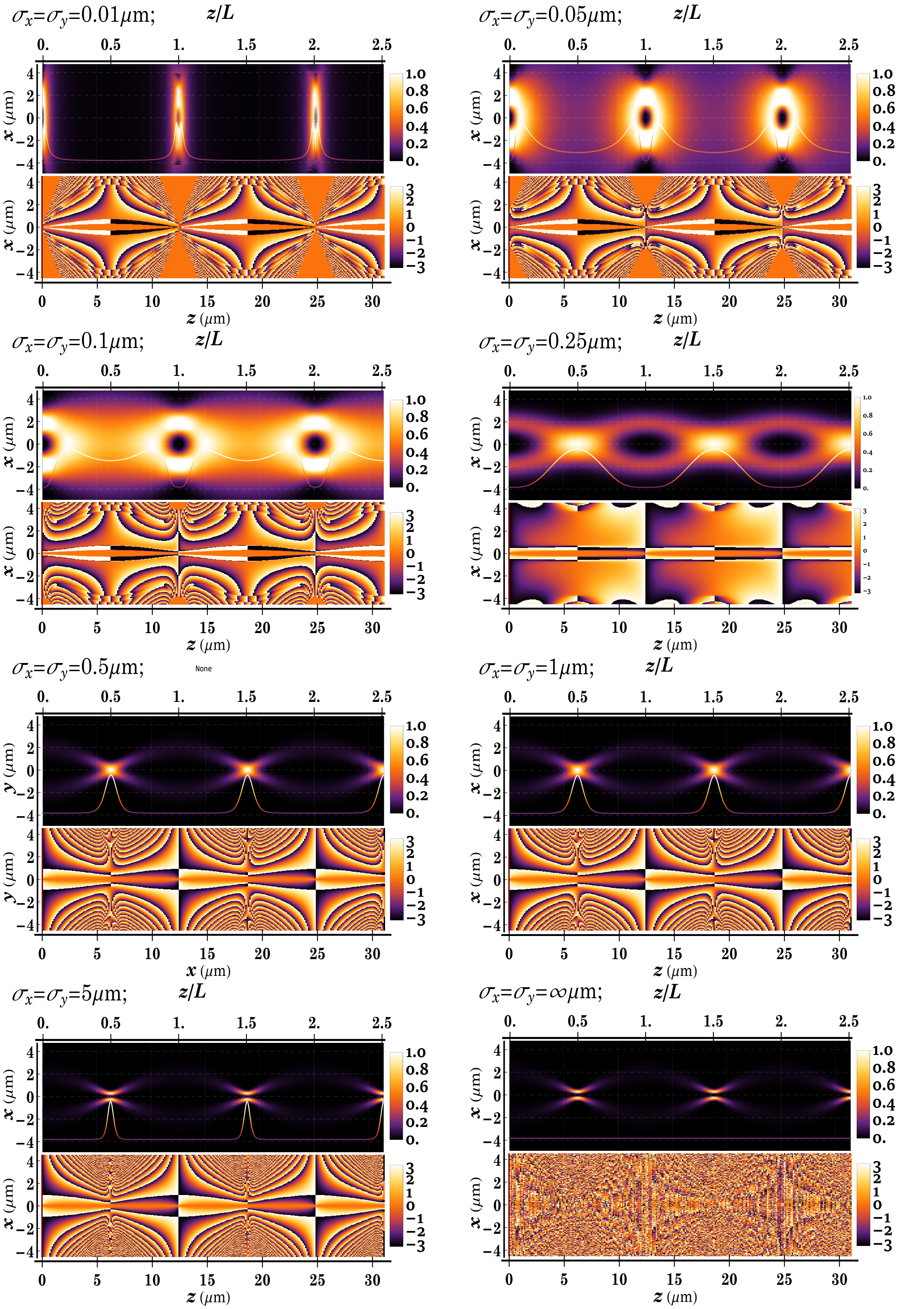

Figure 5. Normalized intensity and the phase distribution of the CSD function for partially coherent Lorentz-Gauss vortex beams propagating through the gradient-index medium with different values of $\sigma_x = \sigma_y$.

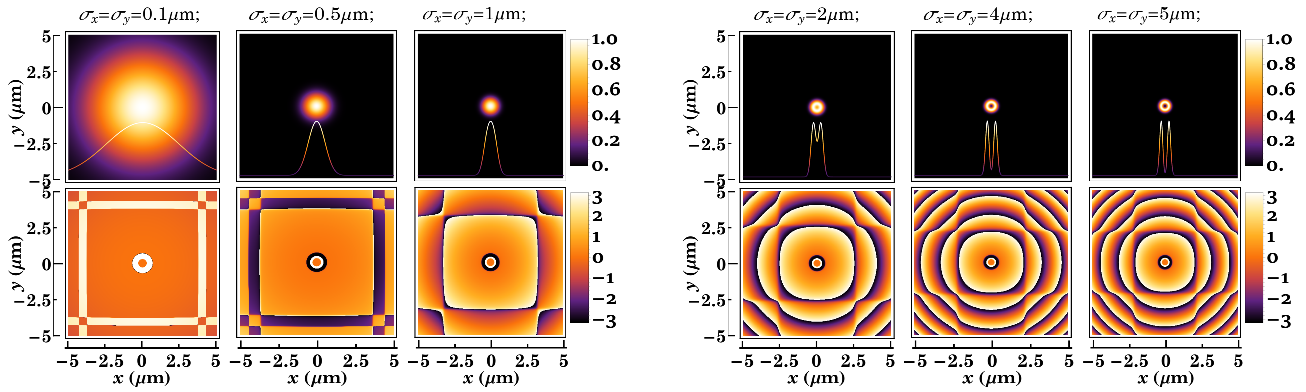

Figure 6. Normalized intensity and the phase distribution of the CSD function for partially coherent Lorentz-Gauss vortex beams propagating through the gradient-index medium With different values of $\sigma_x = \sigma_y$ at $z = 6.25$ μm.

It can be found that the dark spot and the intensity width increase when $w_{0x} = w_{0y}$ increases, and these are when the increase by $w_{0x} = w_{0y}$ is less or equal to w_0, while when $w_{0x} = w_{0y}$ is greater than w_0, there is no effect of intensity along the z-axis. There is a uniqueness at $z = 2\pi$, and at this distance, the dark spot decreases in the middle of the intensity and the intensity width decreases with the increase of $w_{0x} = w_{0y}$. To illustrate further, Fig. 4 displays the contour graph of the distribution of the intensity and phase distribution of the partially coherent Lorentz-Gauss vortex beams propagating in the gradient-index medium at $z = 6.25$ μm with different $w_{0x} = w_{0y}$. We note that in the phase in which $w_{0x} = w_{0y}$ is less than w_0, the phase appears as quadruple rings, while when $w_{0x} = w_{0y}$ is greater than w_0, the mid-phase ring appears circular, while the rings surrounding it are irregularly shaped. All loops appear circular and regular when $w_{0x} = w_{0y} = 10$, and the number of loops increases when $w_{0x} = w_{0y}$ increases.

Figure.5 shows the effect of different coherence lengths σ on the spectral degree of coherence of partially coherent Lorentz-Gauss vortex beams at different distances z in the gradient-index medium. One can see that the greater the coherence length, the greater the intensity a bonding of partially coherent Lorentz-Gauss vortex beams in the gradient-index medium, and in values greater than $\sigma = 5$, with increasing cohesion length, the intensity of the beam is not affected. Similarly, phase cohesion increases with increasing the coherence length and is not affected by large values of bonding length.To illustrate further, Fig. 6 displays the contour graph of the distribution of the intensity and phase distribution of the partially coherent Lorentz-Gauss vortex beams propagating in the gradient-index medium at $z = 6.25$ μm with different σ. One can see from these figures that when the cohesion length is less than or equal to one, the cohesion decreases, the width of the intensity increases, and there is no dark spot as the length of the bonding decreases. When the length of the cohesion is greater than one, the bonding increases and the width of the intensity decreases, and the dark spot grows in the middle of the intensity with increasing the length of the cohesion, while the phase increases the number of rings and becomes irregular in shape approximately as the value of the cohesion length increases.

Figure.7 shows the distribution of the normalized intensity and phase of partially coherent Lorentz-Gauss vortex beams propagating through the gradient-index medium in the x-z plane $(y = 0)$ with different values of β . As can be seen, the parameter β alone establishes the periodic value; it has no effect on the beam width or dark center. The evolution period of the partially coherent Lorentz-Gauss vortex beams in the gradient-index medium reduces with increasing parameter β. While the period of beam evolution increases when β decreases. We can see in Fig. 7 that the phase is not affected by β but the number of cycles for both phase and intensity of partially coherent Lorentz-Gauss vortex beams propagating through the gradient-index medium.

3. CONCLUSION

In this paper, the theory of coherence is used to introduce the partially coherent Lorentz-Gauss vortex beam in a gradient-index medium. The extended Huygens-Fresnel diffraction integral is then used to discuss the evolution properties of the partially coherent Lorentz-Gauss vortex beam propagating in a gradient-index medium. The findings indicate that the black spot in the middle of the Lorentz-Gauss vortex beam gradually grows as M increases and continues to propagate periodically in the direction of z. As the coherence length σ drops, the beam width increases and the black spot gets smaller proportionately. Furthermore, it is discovered that as parameters σ and M decrease, the beam loses its black spot and changes into a Lorentz-Gauss-like beam. In addition, the phase does not change significantly with a change in $w_{0x} = w_{0y}$, σ, or β, while it changes with a change in M. Also, the shape of the phase depends on the values of M if they are odd, the shape of the phase

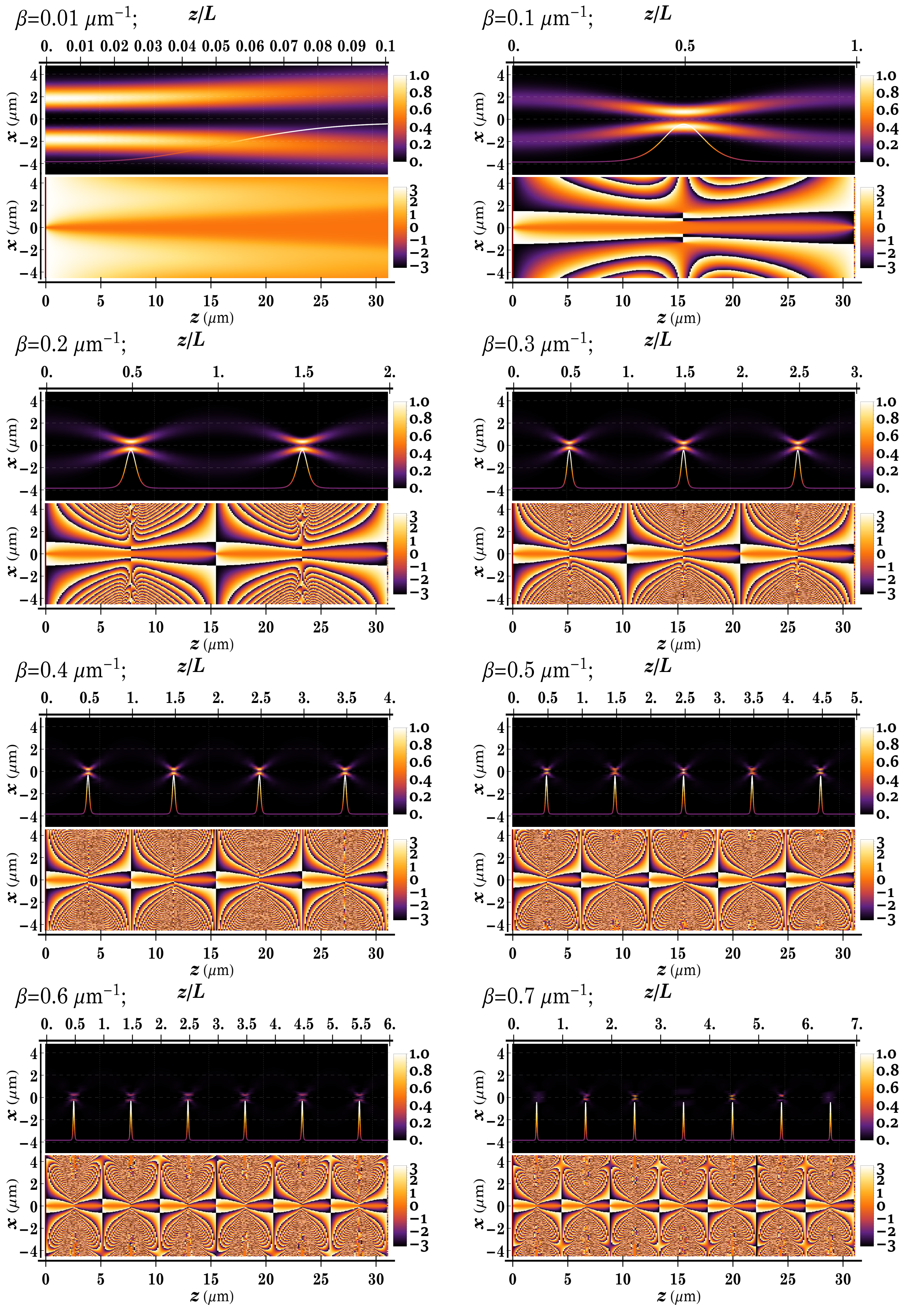

Figure 7. Normalized intensity and the phase distribution of the CSD function for partially coherent Lorentz-Gauss vortex beams propagating through the gradient-index medium with different values of β.

differs from the even M values. While the gradient-index medium parameter β affects the periodic propagation of the beam in the medium, parameter β alone establishes the periodic value with a periodical distance of $L = \pi/\beta$; it has no bearing on the beam's breadth or the black spot. The results of this paper can use in partially coherent Lorentz-Gauss vortex beam optical communication, optical trapping, and fiber communications.

REFERENCES

[1] C. Zhao and Y. Cai, "Paraxial propagation of lorentz and lorentz–gauss beams in uniaxial crystals orthogonal to the optical axis," J. Mod. Opt. **57**, 375–384 (2010).

[2] G. Zhou and X. Chu, "Average intensity and spreading of a lorentz-gauss beam in turbulent atmosphere," Opt. express **18**, 726–731 (2010).

[3] A. A. Alkelly and L. F. Hassan, "Coherence properties and intensity distribution of a partially coherent lorentz–gauss beam emerging from the axicon," Int. J. Opt. **2021**, 1–11 (2021).

[4] H.-P. ZHENG, R.-P. CHEN, and C. H. R. Ooi, "Self-focusing dynamics of lorentz-gaussian beams in kerr media." Lasers Eng. (Old City Publ. **24** (2013).

[5] G. Zhou and G. Ru, "Propagation of a lorentz-gauss vortex beam in a turbulent atmosphere," Prog. In Electromagn. Res. **143**, 143–163 (2013).

[6] M. S. Qusailah, A. A. Alkelly, W. A. Al-Bahry *et al.*, "The propagation properties of a lorentz–gauss vortex beam in a gradient-index medium," Int. J. Opt. **2023** (2023).

[7] H. AL-Nadary, A. A. Alkelly, M. Khaled, and L. F. Hassan, "The effective beam width of a partially coherent rectangular mul-ti-gaussian schell-model vortex beam propagating in a turbulent plasma," Sana'a Univ. J. Appl. Sci. Technol. **1** (2023).

[8] S. Dalgac and K. Elmabruk, *The Propagation of Vortex Beams in Random Mediums*, article 101061 (IntechOpen, 2021).

[9] D. Liu, H. Yin, G. Wang, and Y. Wang, "Propagation of partially coherent lorentz–gauss vortex beam through oceanic turbulence," Appl. optics **56**, 8785–8792 (2017).

[10] Y. Ni and G. Zhou, "Propagation of a lorentz–gauss vortex beam through a paraxial abcd optical system," Opt. Commun. **291**, 19–25 (2013).

[11] D. Liu, H. Yin, G. Wang, and Y. Wang, "Propagation properties of a partially coherent lorentz beam in uniaxial crystal orthogonal to the optical axis," JOSA A **34**, 953–960 (2017).

[12] S. Yang, J. Wang, M. Guo, *et al.*, "Propagation properties of gaussian vortex beams through the gradient-index medium," Opt. Commun. **465**, 125559 (2020).

[13] M. Dong, Y. Bai, J. Yao, *et al.*, "Propagation properties of partially coherent modified bessel–gauss beams through the gradient-index medium," Appl. Opt. **59**, 8023–8028 (2020).

[14] M. Lazrek, Z. Hricha, and A. Belafhal, "Propagation of vortex hermite-cosh-gaussian beams in a gradient-index medium," Opt. Quantum Electron. **54**, 67 (2022).

[15] R. Zhao, F. Deng, W. Yu, *et al.*, "Propagation properties of airy–gaussian vortex beams through the gradient-index medium," JOSA A **33**, 1025–1031 (2016).

[16] Z. Cao, C. Zhai, S. Xu, and Y. Chen, "Propagation of on-axis and off-axis bessel beams in a gradient-index medium," JOSA A **35**, 230–235 (2018).

[17] D. Liu and Y. Wang, "Evolution properties of a radial phased-locked partially coherent lorentz-gauss array beam in oceanic turbulence," Opt. & Laser Technol. **103**, 33–41 (2018).

[18] D. Liu, G. Wang, and Y. Wang, "Average intensity and coherence properties of a partially coherent lorentz-gauss beam propagating through oceanic turbulence," Opt. & Laser Technol. **98**, 309–317 (2018).

[19] A. Jeffrey and H. H. Dai, *Handbook of mathematical formulas and integrals* (Elsevier, 2008).

[20] I. S. Gradshteyn and I. M. Ryzhik, *Table of integrals, series, and products* (Academic press, 2014).

[21] G. Zhou, "Propagation of a partially coherent lorentz-gauss beam through a paraxial abcd optical system," Opt. Express **18**, 4637–4643 (2010).